NANO LETTERS

2005
Vol. 5, No. 10
2112−2115

Dielectrophoretically Controlled Fabrication of Single-Crystal Nickel Silicide Nanowire Interconnects

Lifeng Dong, Jocelyn Bush, Vachara Chirayos, Raj Solanki, and Jun Jiao*

Department of Physics, Portland State University, Portland, Oregon 97207-0751

Yoshi Ono, John F. Conley, Jr., and Bruce D. Ulrich

Integrated Circuit Process Technology Group, Sharp Labs of America, Camas, Washington 98607

Received August 19, 2005; Revised Manuscript Received September 12, 2005

ABSTRACT

We report here on applying electric fields and dielectric media to achieve controlled alignment of single-crystal nickel silicide nanowires between two electrodes. Depending on the concentration of nanowire suspension and the distribution of electrical field, various configurations of nanowire interconnects, such as single, chained, and branched nanowires were aligned between the electrodes. Several alignment mechanisms, including the induced charge layer on the electrode surface, nanowire dipole–dipole interactions, and an enhanced local electrical field surrounding the aligned nanowires are proposed to explain these novel dielectrophoretic phenomena of one-dimensional nanostructures. This study demonstrates the promising potential of dielectrophoresis for constructing nanoscale interconnects using metallic nanowires as building blocks.

In an integrated circuit (IC), the function of an interconnect is to distribute signals as well as to supply power to the active components on a chip. As device dimensions are scaled down and the chip device density increases, interconnects play a critical role in overall device performance. When downscaling interconnect dimensions smaller than the electron mean free path of metallic conductors, two main concerns are to maintain low resistance and to minimize electromigration (EM) related failure due to increased current density. Maintaining low resistance is a challenge because when the pitch approaches tens of nanometers, the resistance typically increases due to interface, grain boundary, and surface roughness induced carrier scattering.[1,2] The other issue when reducing the cross-sectional area of an interconnect is the increase in its current density, J, which reduces its lifetime due to EM-related failure. Hence, it is essential to explore conductor materials that can solve these problems and are, therefore, suitable for future generations of nanoscale devices. Currently, copper (Cu) is utilized in electronic devices for contacts and local interconnects. In comparison to Cu, NiSi appears to be a suitable candidate for fabricating nanoscale interconnects due to its small carrier scattering mean free path. The mean free paths of Cu and NiSi have been estimated to be about 40 and 5 nm, respectively.[1−3] Since EM is driven by grain boundaries, it is expected that elimination of EM could be achieved by using high-quality single-crystal NiSi nanowire interconnects. Recently, a remarkably high J_{max}, on the order of 10^9 A·cm^{-2}, was reported for single-crystal NiSi nanowires.[3] Considering the above factors, single-crystal NiSi nanowires appear to be very attractive candidates for future interconnect applications.

In the past few years, dielectrophoresis has been utilized to align metallic nanowires and carbon nanotubes between electrodes.[4−9] However, no systematic studies have been done on the interaction among nanowires or nanotubes during the dielectrophoresis process or the interaction between the aligned nanostructures and substrates. In this paper, we demonstrate a systematic investigation of these interactions and provide explanations for the interaction mechanisms and ultimately develop an effective dielectrophoresis method for constructing NiSi nanowire-based networks of interconnects.

The NiSi nanowires used in this study were synthesized by the decomposition of silane on nickel substrates as described elsewhere.[10] The nanowires were annealed at 600 °C (in forming gas) to ensure the proper phase of the silicide. To prepare the nanowire suspension for dielectrophoresis experiments, a piece of nickel substrate with synthesized NiSi nanowires was placed into a vial filled with ethanol solution and then sonicated for 5 min. The sonication allows the nanowires to be removed from the nickel substrate and dispersed in the ethanol solution. After the sonication, the upper 80% of the clean supernatant was decanted for

* Corresponding author. E-mail: jiaoj@pdx.edu.

10.1021/nl051650+ CCC: $30.25
Published on Web 09/27/2005

dielectrophoresis experiments. During the dielectrophoresis experiments, 3 μL of the nanowire suspension was dropped onto the region between two electrodes and an external voltage (10 Vp-p, 10 MHz) was applied for 30 s. The patterned platinum (Pt) electrodes (120-nm thickness) with gap distances ranging from 0.5 to 2.5 μm were fabricated on a silicon substrate covered with a thermal oxide layer (1-μm thickness). A 50 nm thick titanium nitride (TiN) layer was used to promote the adhesion of the Pt film to the oxide layer. Then, the substrates with aligned nanowires were soaked in deionized water for 15−20 min, rinsed with deionized water, and dried with flowing nitrogen gas.

An FEI Sirion field emission scanning electron microscope (SEM) was utilized to characterize the morphology and orientation of nanowires aligned between two electrodes. During the imaging, an acceleration voltage of 1 or 2 kV was used to minimize the irradiation of the electron beam on the nanowire surfaces. An FEI Tecnai F20 transmission electron microscope (TEM) was employed to study the internal structure of the nanowires. TEM samples were prepared by dropping a 3-μL nanowire suspension onto a copper grid coated with a thin carbon film. The TEM image in Figure 1a shows that the nanowires have smooth surface and uniform diameters ranging from 15 to 20 nm. The image also suggests that these randomly oriented nanowires are not bundled, although they are piled together on the TEM grid. Their distribution phenomena are very similar to that of multiwalled carbon nanotubes. This is in contrast to the bundled single-walled carbon nanotubes which are bonded together by van der Waals force.[11] The high-resolution TEM image in Figure 1b and its corresponding two-dimensional fast Fourier transform (FFT) pattern clearly indicate that the NiSi nanowires are single crystal with very little (<1 nm) amorphous coating, and the nanowires grow along the [001] direction.

In general, a dielectrophoresis experiment could be conducted using either direct current (dc) or alternating current (ac) electrical fields.[12,13] However, in our case, we found that at a frequency lower than 50 kHz, electrolysis occurred and destroyed the surface of the electrodes. When we used an electrical field of 10 V_{p-p} at a frequency of 10 MHz, as demonstrated in Figure 2a, NiSi nanowires were well-aligned along the electrical field lines between the electrodes. Note that nanowires were asymmetrically distributed between the two electrodes and were only attracted toward the top electrode when a sinusoidal ac potential was supplied. The bottom electrode was kept grounded during the dielectrophoresis experiments. It is also apparent that, in the center of the two electrodes, several nanowires were aligned on top of both electrodes. When the nanowire concentration was further decreased, an individual nanowire could be aligned onto the center region of the two electrodes as shown in Figure 2b and its magnified portion (Figure 2c). Note that both ends of the nanowire were attached to the electrodes. The mechanism for controlled dielectrophoretic positioning of nanowires on top of the electrodes could be explained by the schematic diagram in Figure 2d. In a simple case, a nanowire is floating above two electrodes with its

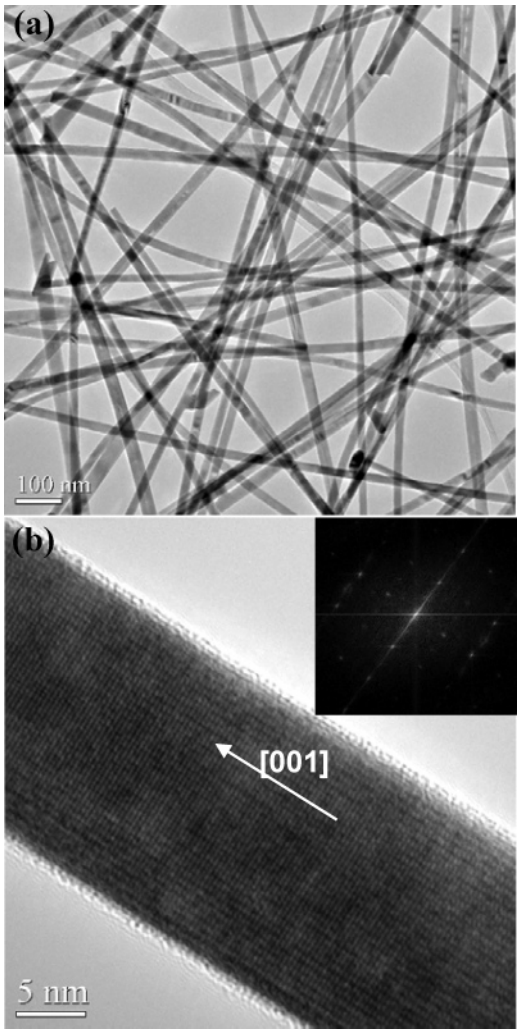

Figure 1. (a) TEM image of NiSi nanowires with diameters ranging from 15 to 20 nm. (b) A high-resolution TEM image and its corresponding FFT (inset) indicate the nanowires are single crystal and grow along the [001] direction.

longitudinal axis parallel to the electrode axis. Since the right-hand side electrode is kept grounded, an induced charge layer only exists on the left-hand side electrode. As illustrated in Figure 2d, the dielectrophoretic force on the induced dipole within the nanowire has a tangential component, F_x, parallel to the surface of the electrodes; thus, one end of the nanowire was positioned on the surface of the electrode. For instance, when the left-hand side electrode is provided with a positive potential, negative charges are induced in the left ends of the nanowires; the nanowires are then attracted onto the surface of the electrode. During the dielectrophoretic positioning, the orientation of nanowires is controlled by the torque, $\vec{T}$, exerted on the induced electrical dipole moment, $\vec{P} = q\vec{d}$

$$\vec{T} = \vec{P} \times \vec{E} = q\vec{d} \times \vec{E} \tag{1}$$

where q is the induced electrical charge on the nanowire, $\vec{d}$ is the displacement between the induced charges, and $\vec{E}$ is the electrical field. Notice that the direction of torque, $\vec{T}$, depends on the electrical field vector, $\vec{E}$. In an electrical field,

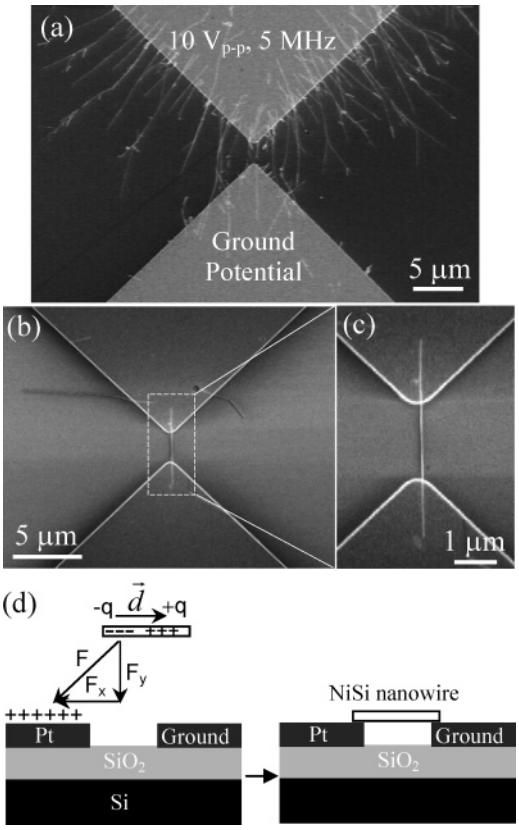

Figure 2. (a) A number of NiSi nanowires were aligned through dielectrophoresis between two Pt electrodes. (b) With the proper control of nanowire concentration in the suspension, a single NiSi nanowire was aligned between electrodes. (c) This is a further magnified image from the area marked in (b). (d) A diagram is illustrated to show that the dielectrophoresis positioning of a nanowire above the electrode results from the charge layer on the electrode surface.

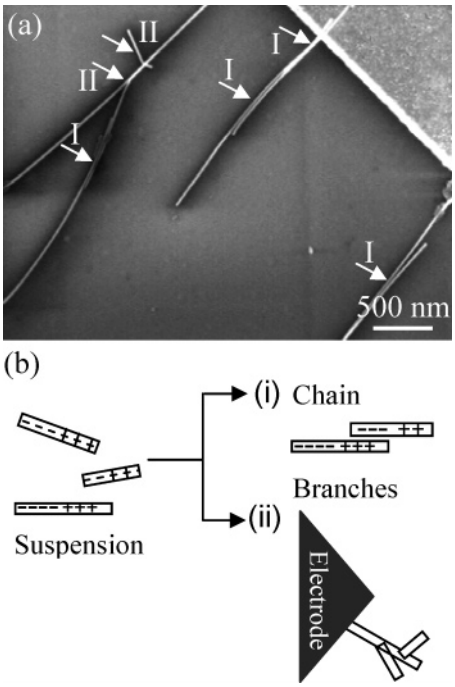

Figure 3. (a) A high-magnification SEM image of chained and branched NiSi nanowires. (b) Schematic diagrams illustrate the formation processes of these two novel dielectrophoretic phenomena, which result from the dipole−dipole interaction and the enhanced electrical field surrounding the aligned nanowires, respectively.

the torque aligns the longitudinal axis of a nanowire parallel to the direction of the electrical field, then $\vec{T}$ reduces to zero when $\vec{d}$ is parallel to $\vec{E}$. Therefore, as demonstrated in Figure 2a, when the nanowires were moved toward the top electrode, the direction of movement was along the electrical field, which was along the radial direction of the top electrode. If the length of a nanowire were greater than the gap between two electrodes, it could sit on the top of both electrodes as demonstrated in Figure 2a and Figure 2b.

We also observed other structural branching phenomena as shown in Figures 2a and 3a. During dielectrophoretic alignment, chains of nanowires as well as Y-shaped branches were formed, though the nanowires were well separated through sonication in the ethanol solution (Figure 1). This means that the dielectrophoretic process not only can position individual nanowires between two electrodes but also can form nanowire networks. This structural phenomenon could allow the transport of signals from one component to a number of other connected components, an important requirement for the practical applications of conducting interconnects. To explain these novel structural phenomena, two alignment models are proposed and schematically illustrated in Figure 3b. When an external electrical field is applied onto the nanowire suspension, nanowires are polarized with dipoles induced within the wire and aligned along the electrical field direction by the electrical torque. Then, due to the Coulomb force, if the neighboring nanowires are close enough to be electrically attracted, polarized nanowires attract the neighboring nanowires to form chains parallel to their long axes, as demonstrated by the nanowire chain marked as I in Figure 3a. The newly formed chain was then positioned by dielectrophoresis onto the top of an electrode's edge in the direction of the electrical field. This proposed mechanism can be supported by more results listed in the Supporting Information (Figure S1). While a nanowire or a nanowire chain is positioned on top of the electrodes, a strong electrical field around the nanowire tips is induced by the nanowires' high aspect ratio and small radius. The enhanced electrical field around the tips of one-dimensional nanostructures, such as carbon nanotubes[14,15] and ZnO nanowires,[16] has been demonstrated through studies of their electron field emission behaviors. The surrounding nanowires in the suspension tend to align along the radial directions of the nanowire to form nanowire branches. This phenomenon is illustrated in Figure 3b and demonstrated by the nanowire branches labeled as II in Figure 3a. Further verifications of this phenomenon are provided in the Supporting Information (Figure S2).

To study the interaction between NiSi nanowires and the electrode surface, we used a two-probe method to measure electrical resistances of single nanowires aligned between two Pt electrodes. One electrode was common (0 V), and the other one was swept from −2 to 2 V in steps of 0.1 V. We measured more than 40 individually aligned nanowires

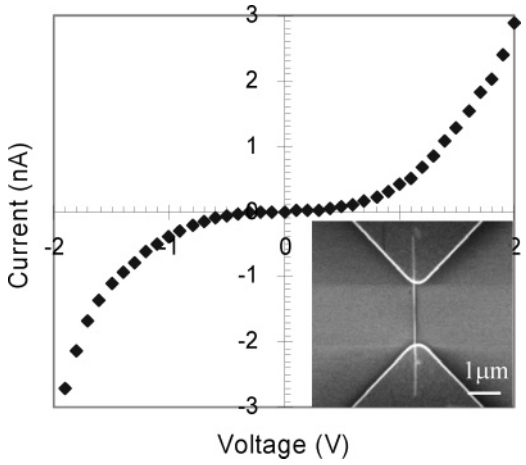

Figure 4. *I*−*V* behavior of a single NiSi nanowire aligned on top of two electrodes after electron beam irradiation of its contact areas with the electrodes. Inset is the nanowire SEM image.

under the condition that no extra metal layer was deposited on top of the aligned nanowires in the electrode area. Out of 40 nanowires, none showed a detectable current signal above the noise background at picoampere levels. The low current signals could be caused by (1) potential barriers of carrier transport at the interface between the aligned nanowires and the surface of Pt electrodes, such as an oxidation layer on the nanowire or electrode surface, or (2) a weak physical contact between the nanowires and the electrode surfaces. To remove the oxidation top layers, the samples with the aligned nanowires were annealed at 450−600 °C and in forming gas (N_2/H_2) for 60 s. However, there were still no detectable signals after the annealing process. In another attempt to improve the physical contact between the nanowire and the electrode surfaces, we used an electron beam to irradiate both ends of the nanowires during SEM characterization after the first electrical measurement. A typical *I*−*V* curve in Figure 4 demonstrates that currents of several nanoamperes were obtained from the nanowires after the electron-beam irradiation on their contact areas with the electrodes. Similar experimental results were observed when we utilized focused ion beam (FIB) techniques to deposit a Pt layer on the top of each end of the aligned nanowires. The detailed FIB-induced Pt deposition parameters have been described elsewhere.[17] The low current signals obtained prior to irradiation are likely the result of loose contact between the nanowire and the Pt electrode. However, the nonlinear *I*−*V* behavior in Figure 4 shows that there are still potential barriers to carrier transport between the nanowire and the Pt electrode, even after the process of electron beam irradiation or FIB-induced Pt deposition. This means the nonlinear electrical behavior was the result of the contact resistances between the aligned nanowire and the electrode surface. This kind of electrical transport phenomenon also occurs at the contact region between carbon nanotubes and metal electrodes, such as Au and Pt.[18,19]

In conclusion, a simple and effective dielectrophoresis method was demonstrated to fabricate single NiSi nanowire interconnects. Branches as well as chains of NiSi nanowire interconnects were also obtained. During the dielectrophoresis alignment, nanowires were positioned on top of electrodes due to an induced charge layer on the electrode surface. When electrical potential was applied to the nanowire suspension, some nanowires formed a chain with neighbor nanowires as a result of the dipole−dipole interaction. After single nanowires or chains of nanowires were aligned, the electrical field surrounding these nanowires was enhanced; some nanowires in the suspension were attracted to these stem nanowires to form branches. These important structural phenomena show great potential for developing controlled dielectrophoretic procedures to fabricate nanoscale metal interconnects.

Acknowledgment. This research was financially supported by Sharp Labs of America and the National Science Foundation (DMR-220926). The authors thank William K. Meyer and Cheng Qi for their help with the use of electrical characterization facilities.

Supporting Information Available: More high-resolution SEM images showing a large number of adjacent chains and branching sites. This material is available free of charge via the Internet at http://pubs.acs.org.

References

(1) Rossnagel, S. M.; Kuan, T. S. *J. Vac. Sci. Technol., B* **2004**, *22*, 240.
(2) Steinhögl, W.; Schindler, G.; Steinlesberger, G.; Engelhardt, M. *Phys. Rev. B* **2002**, *66*, 075414.
(3) Wu, Y.; Xiang, J.; Yang, C.; Lu, W.; Lieber, C. M. *Nature* **2004**, *430*, 61.
(4) Smith, P. A.; Nordquist, C. D.; Jackson, T. N.; Mayer, T. S.; Martin, B. R.; Mbindyo, J.; Mallouk, T. E. *Appl. Phys. Lett.* **2000**, *77*, 1399.
(5) Fan, D. L.; Zhu, F. Q.; Cammarata, R. C.; Chien, C. L. *Appl. Phys. Lett.* **2004**, *85*, 18.
(6) Chen, X. Q.; Saito, T.; Yamada, H.; Matsushige, K. *Appl. Phys. Lett.* **2001**, *78*, 3714.
(7) Krupke, R.; Hennrich, F.; LÖhneysen, H. v.; Kappes, M. M. *Science* **2003**, *301*, 344.
(8) Krupke, R.; Hennrich, F.; Weber, H. B.; Kappes, M. M.; Löhneysen, H. v. *Nano Lett.* **2003**, *3*, 1019.
(9) Dong, L. F.; Chirayos, V.; Bush, J.; Jiao, J.; Dubin, V. M.; Chebian, R. V.; Ono, Y.; Conley, J. F., Jr.; Ulrich, B. D. *J. Phys. Chem. B* **2005**, *109*, 13148.
(10) Decker, C. A.; Solanki, R.; Freeouf, J. L.; Carruthers, J. R.; Evans, D. R. *Appl. Phys. Lett.* **2004**, *84*, 1389.
(11) O'Connell, M. J.; Bachilo, S. M.; Huffman, C. B.; Moore, V. C.; Strano, M. S.; Haroz, E. H.; Rialon, K. L.; Boul, P. J.; Noon, W. H.; Kittrell, C.; Ma, J.; Hauge, R. H.; Weisman, R. B.; Smalley, R. E. *Science* **2002**, 297, 593.
(12) Pohl, H. A. *Dielectrophoresis*; Cambridge University Press: Cambridge, U.K., 1978.
(13) Jones, T. B. *Electromechanics of Particles*; Cambridge University Press: Cambridge, U.K., 1995.
(14) Jonge, N.; Schoots, K.; Oosterkamp, T. H. *Nature* **2002**, *420*, 393.
(15) Dong, L. F.; Jiao, J.; Pan, C. C.; Tuggle, D. W. *Appl. Phys. A* **2004**, *78*, 9.
(16) Dong, L. F.; Jiao, J.; Tuggle, D. W.; Petty, J. M.; Elliff, S. A.; Coulter, M. *Appl. Phys. Lett.* **2003**, *82*, 1096.
(17) Jiao, J.; Dong, L. F.; Foxley, S.; Mosher, C. L.; Tuggle, D. W. *Microsc. Microanal.* **2003**, *9*, 516.
(18) Javey, A.; Guo, J.; Wang, Q.; Lundstrom, M.; Dai, H. J. *Nature* **2003**, *424*, 654.
(19) Heinze, S.; Tersoff, J.; Martel, R.; Derycke, V.; Appenzeller, J.; Avouris, Ph. *Phys. Rev. Lett.* **2002**, *89*, 106801.

NL051650+